

## Mechanical and Electrical Properties of TiO<sub>2</sub> Loaded Vulcanized Natural Rubber

M.A. Sulaiman<sup>1,\*</sup>, W. Panwiriyarat<sup>2</sup>, B.L.C. Jie<sup>1</sup>, M.N. Masri<sup>1</sup>, M. Yusuff<sup>1</sup>

<sup>1</sup>Advanced Materials Research Cluster, Faculty of Earth Science, Universiti Malaysia Kelantan, 17600 Jeli, Kelantan, Malaysia,

<sup>2</sup>Faculty of Science and Industrial Technology, Prince of Songkla University, Surat Thani Campus, Surat Thani 84000, Thailand.

\*E-mail Address: azwadi@umk.edu.my

Received: 2 December 2016 / Accepted: 30 December 2016 / Published: 31 December 2016

**ABSTRACT:** High dielectric constant material is very important to miniaturize many electronic devices. TiO based ceramics are well-known materials due to the very high dielectric constant at room temperature and nearly independence within wide frequency range. However, forming process for the ceramic into the desired shape requires pressing and sintering and these will limit the control for the complex shapes. To overcome this problem, it is very useful to produce composite from TiO<sub>2</sub> powder with polymer. Among the polymer class material, elastomer type such as Vulcanized Natural Rubber (VNR) indicates very high flexibility and robust. Processing of TiO<sub>2</sub>/VNR composite involved vulcanization of rubber and followed by compounding with TiO<sub>2</sub> (0, 5, 10, 20, 30 and 50 phr) in an internal mixer. Small blocks of composites were produced after compression using moulding machines and characterized for mechanical, microstructural and electrical properties. Mechanical testing of the composites indicates that high TiO<sub>2</sub> content causes tensile strength starts to increase. Impedance spectroscopy measurement also shows that the increasing of TiO<sub>2</sub> content can improve dielectric constant from 3.1513 to 3.4935 at 175 kHz and dielectric loss is decreasing from 0.0323 to 0.0252 at 1.2775 MHz. Microstructure of the composite was observed, and crystal of TiO<sub>2</sub> immersed in the VNR with good surface contact.

**Keywords:** Dielectric material; Rubber/ceramic composite; Vulcanized natural rubber

### 1. Introduction

Traditional polymer materials may exhibit high mechanical properties but have a relatively low dielectric constant ( $\epsilon_r < 10$ ) [1,2]. To increase the dielectric constant for better applications, polymer materials are used as a matrix in composite with materials, which has a high dielectric constant as fillers [3–5]. Compared to CaCu<sub>3</sub>Ti<sub>4</sub>O<sub>12</sub> [6,7] or BaTiO<sub>3</sub> [8,9], TiO<sub>2</sub> has lower but still relatively high dielectric constant value ( $\epsilon_r > 60$ ) among the binary metal oxides [10,11]. However, it has a rigid anatase structure at a low temperatures [12]. Hence, another material is needed to provide the necessary mechanical properties. These needed properties can be found in natural rubber that has suitable mechanical and physical properties such as low temperature flexibility, high elasticity and fatigue resistance [13]. However, it is important to identify the weight percentage of TiO<sub>2</sub> to be used as filler in natural rubber composite as high filler loading might decrease the mechanical properties of the natural rubber composite while low filler loading might cause dielectric constant has no significant effect. This research's aim is to produce TiO<sub>2</sub>/Rubber composites to combine the beneficial properties of each of the materials such as mechanical and electrical properties.

### 2. Experimental

TiO<sub>2</sub> loaded vulcanized natural rubber (VNR) was prepared by mixing natural rubber, sulphur, zinc oxide, stearic acid, mercaptobenzothiazole (MBT) and TiO<sub>2</sub> based on phr formulation 100, 3.5, 0.6, 0.5 and  $x$  ( $x = 0, 5, 10, 20,$

30 and 50) respectively. The formulated raw materials excluded sulphur and MBT were incorporated into the internal mixer for 5 minutes at 160°C. The sulphur and MBT was mixed later using two-roll mill for 1 and 2 minutes respectively. The rubber compound was sheeted out, spread with talcum powder and left at room temperature for 24 hours for material's characterization. Mechanical properties were determined using Tinius Olsen Testing Machine. Thin sheets of composites were cut to 4 small dumb bell-shaped samples of ASTM die type C. The grip separation speed was set to 500 mm/minute and initial gauge length 20 mm following ASTM D412. The tensile strengths of the compounds are tested with Tinius Olsen tensile test machine. Microstructure of the composites was observed using Scanning Electron Microscope, Quanta400, FEI, Czech Republic and electrical properties were measured using Agilent 4285A Precision LCR Meter at frequency range from 75 kHz to 30 MHz.

### 3. Results and discussions

**Figure 1** shows the stress-strain behaviour of the composite with different load of TiO<sub>2</sub>. All samples exhibit the increasing stress with strain, but a drastic increase is observed when strain is higher than 500%. This occurred as the result of “self-reinforcing” of the rubber caused by a tendency of the network chains of NR that tend to orient themselves in the direction of stretching or force applied leading to formation of crystallites. According to Zhang et al. [14], natural rubber is a crystalline type of polymer. Molecules of rubber will form fixed orientation when

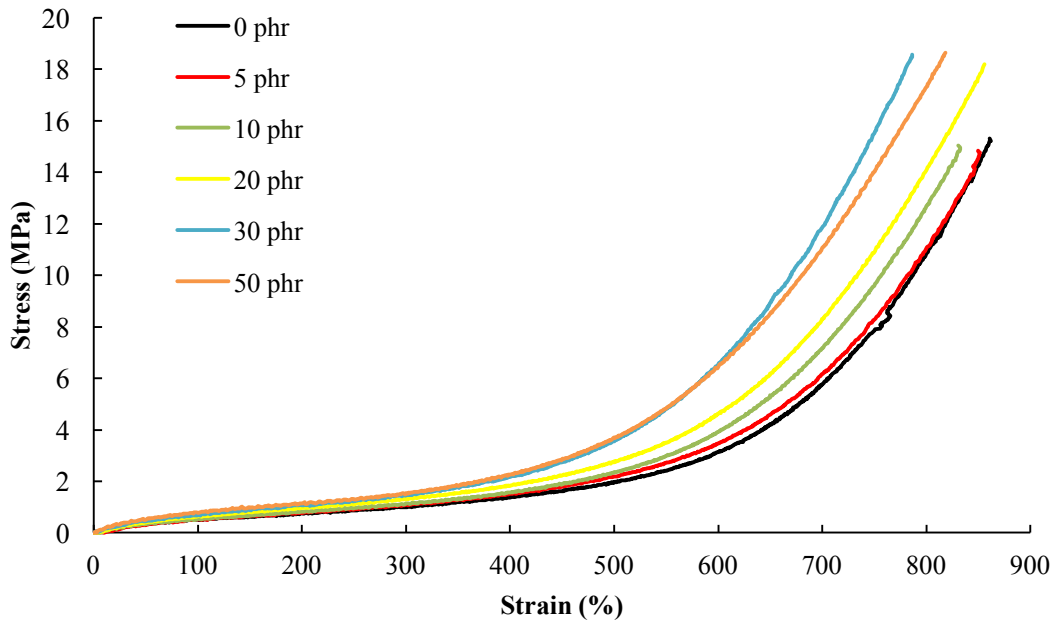


Figure 1: Stress-strain behaviour of composites with different load TiO<sub>2</sub>

stretched and causing polymeric chains of rubber to become narrow. By adding ceramic's filler, it can serve as nucleating agent and causing the molecular chain to become easier to rearrange and formed crystal quickly under stretched. Higher filler content allows higher interaction rubber/filler and increases the reinforcing effects. However, this is only applicable to certain limits of ceramics content [14].

In Figure 2, increasing TiO<sub>2</sub> phr loading of 0, 5, 10, 20 and 30 shows an increasing of tensile strength. However, sample of 50 phr recorded slightly decreased in the tensile strength, and this is believed due to the limits for reinforcing effects. The aggregations of filler (can be seen the microstructure) that existed on the higher filler content create the stress point under a condition of stretch. The motion of rubber molecular chain was constrained, causing the flexibility of composite decreased. Elongation at break

is affected by the same reason as well. Irregular pattern for the elongation at break may be caused by the irregular amount of polymeric chain and crosslink [16]. These are major factors that affecting the elongation at break for VNR. However, the standard deviations can be seen is decreased with the increasing of TiO<sub>2</sub> as shown on the error bar. It is suggested that, higher concentration of TiO<sub>2</sub> replaced the intrinsic properties of irregular polymeric chain and resulting more consistent measurement of their elongation at break.

Figure 3 depicts the dielectric constant of different TiO<sub>2</sub> loaded VNR at frequency 175 kHz to 30 MHz measured using LCR Meter. The dielectric constant is decreasing as frequency increases. The decreases happen as the dipole orientation and displacement polarization could not follow the change of alternation electric field efficiently at higher frequency. This happens to almost all high dielectric

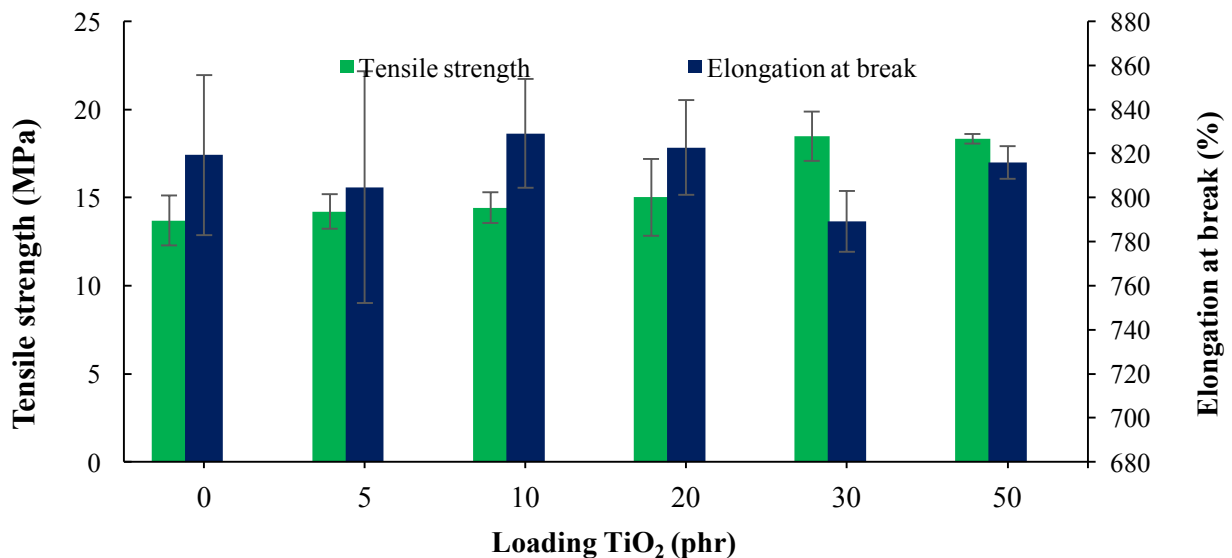


Figure 2: Bar chart of tensile strength and elongation at break at different TiO<sub>2</sub> loading

materials [7,17–19]. Higher TiO<sub>2</sub> loading causes the increasing of dielectric constant as predicted. But the highest TiO<sub>2</sub> sample which is 50 phr is not drastically increasing the dielectric properties to the composite as polycrystalline TiO<sub>2</sub> alone at the same frequency range was reported [20] can spot at ~85 of dielectric constant (1 MHz). The wide difference is due to the polycrystalline of TiO<sub>2</sub> have space charge polarization between the grain boundaries that created Internal Boundary Layer Capacitor (IBLC). At 175 kHz, the dielectric constant is increased from 3.144 for 0 phr to 3.49 for 50 phr. However, for 30 phr and 50 phr, the increasing of the dielectric constant is very

small, which is less than 0.002 as the limit of TiO<sub>2</sub> addition. The limiting factors are unknown and should be further investigated with higher TiO<sub>2</sub> loading composite and circuit equivalence analyses.

Addition of TiO<sub>2</sub> will contribute to increasing polarization amount, which is space charge polarization at the particle-rubber matrix boundary. The increasing of this polarization by adding more TiO<sub>2</sub> will increase the dielectric constant. However, this will affect the mechanical properties as well. More investigation should be conducted, which is involved higher TiO<sub>2</sub> loading to explore the extended properties of the composites.

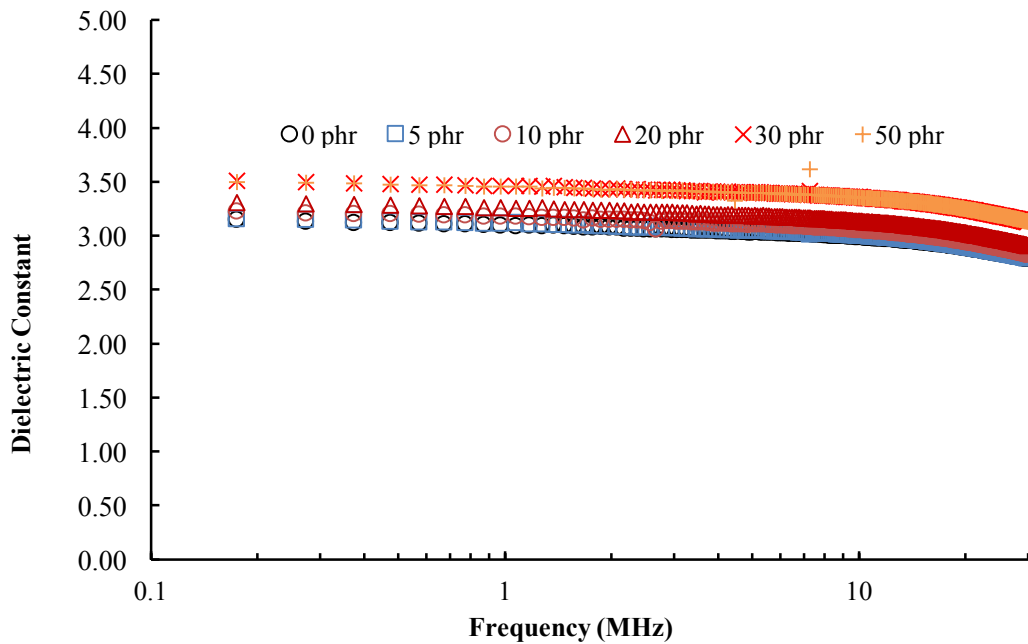


Figure 3: Dielectric constant of different TiO<sub>2</sub> loaded VRN at different frequency range

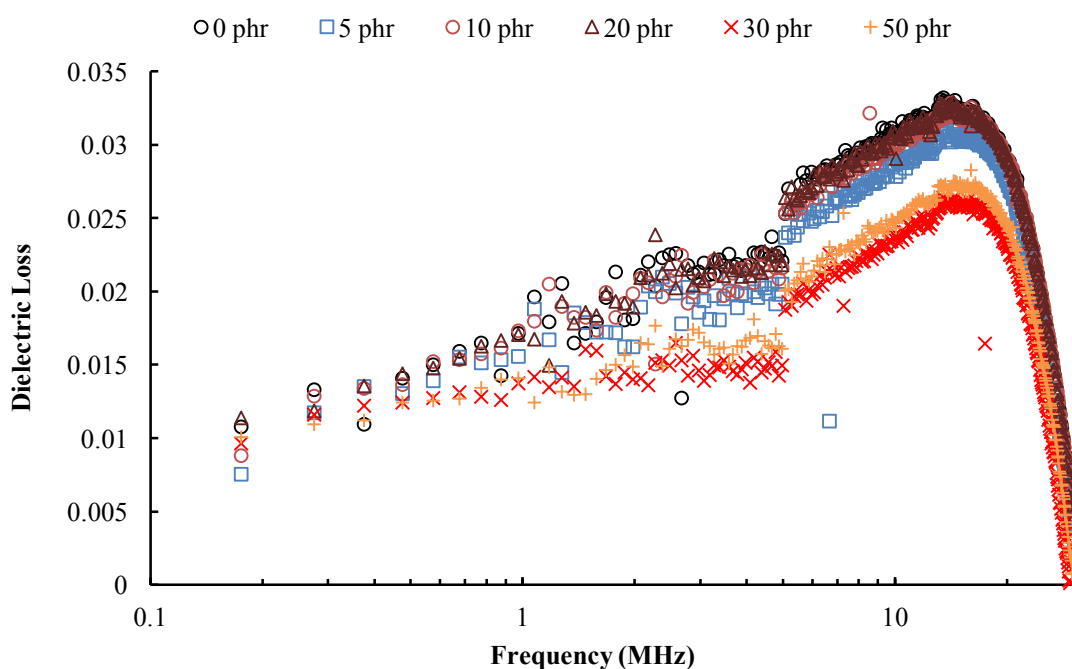
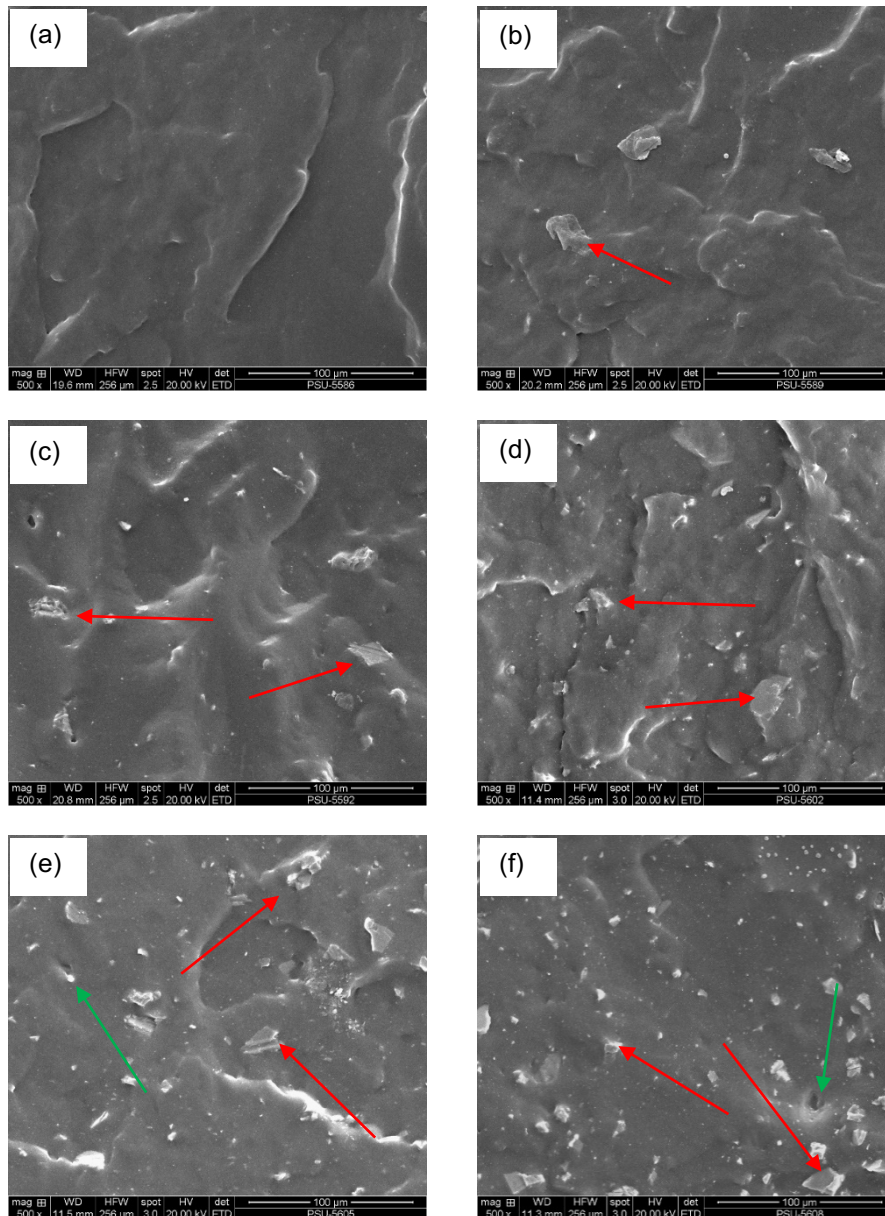


Figure 4: Dielectric loss of different TiO<sub>2</sub> loaded VRN at different frequency range



**Figure 5:** SEM micrographs of  $\text{TiO}_2$ /VNR composites with various  $\text{TiO}_2$  loadings (a) 0, (b) 5, (c) 10, (d) 20, (e) 30 and (f) 50 phr

Dielectric loss of polymeric materials as expected is very low and this is shown in **Figure 4**. The different  $\text{TiO}_2$  loaded VNR was tested their dielectric loss at frequency 175 kHz to 30 MHz, and the value is below 0.0324. The dielectric loss is increasing with frequency is up to 14.5 MHz, and the properties reduced drastically until 0.0008 at 30 MHz. Within 14.5 and 30 MHz, the relaxation phenomenon has occurred, and the effect is also noticed in dielectric constant in Figure 3 as well. The relaxation of dielectric is suggested due to the space-charge polarization has lost effectiveness to catch up the high frequency alternating electric field and revealed the origin intrinsic properties of VNR [13].

**Figure 5** shows the FESEM images for all samples. Visible and homogenous morphologies can be observed in (a) which proves the absence of  $\text{TiO}_2$  additive.  $\text{TiO}_2$  particles are fairly dispersed in (b) and (c) and still have high inter particle distance and low agglomeration. However, from 20 phr onwards, (d), (e) and (f) larger

agglomerated particles of  $\text{TiO}_2$  start to exist. This is due to the decreasing inter particle distance which increases agglomeration of  $\text{TiO}_2$  as shown by the red arrows in (d), (e) and (f). The effect is apparent in (f) shown by the green arrow where porosity starts to occur at 50 phr. This is suggested caused by the decreasing of adhesion between matrix and filler. As the filler loading increases, the thickness of the matrix will decrease due to the density different between  $\text{TiO}_2$  and vulcanized rubber. When higher density of  $\text{TiO}_2$  replaced vulcanized rubber at the same weight, the occupied volume is reduced to the composites.

#### 4. Conclusion

$\text{TiO}_2$  loaded VNR produced have improved the tensile strength and elongation at break become more precise. Dielectric constant was increased by  $\sim 0.3487$  at frequency from 175 kHz to 30 MHz with increasing  $\text{TiO}_2$  concentration up to 50 phr. Observation on the microstructure indicated increasing samples with 20 phr

TiO<sub>2</sub> shows good dispersion and adhesion to the matrix, and porosity started to occur at 50 phr.

#### Acknowledgements

This research work was financially supported by the Ministry of Higher Education (MOHE) through Fundamental Research Grant Scheme (FRGS) R/FRGS/A08.00/00880A/002/2014/000174. Special appreciation to Student Mobility Programme between Faculty of Earth Science, University Malaysia Kelantan and Faculty of Science and Industrial Technology, Prince of Songkla University, Surat Thani Campus for research technical and student welfare supports.

#### References

1. B.C. Huang, Q. Zhang, *Adv. Funct. Mater.* 14 (2004) 501–506.
2. F. Amaral, C.P.L. Rubinger, F. Henry, L.C. Costa, M.A. Valente, A. Barros-Timmons, *J. Non. Cryst. Solids*. 354 (2008) 5321–5322.
3. A. Rajabtabar-Darvishi, W.L. Li, O. Sheikhejad-Bishe, L.D. Wang, Y. Zhao, S.Q. Zhang, W.D. Fei, *J. Alloys Compd.* 514 (2012) 179–182.
4. P. Thomas, K. Dwarakanath, K.B.R. Varma, *Synth. Met.* 159 (2009) 2128–2134.
5. C.C. Wang, Y.J. Yan, L.W. Zhang, M.Y. Cui, G.L. Xie, B.S. Cao, *Scr. Mater.* 54 (2006) 1501–1504.
6. M.A. Sulaiman, S.D. Hutagalung, Z.A. Ahmad, *Adv. Mater. Res.* 364 (2012) 455–459.
7. M.A. Sulaiman, S.D. Hutagalung, Z.A. Ahmad, M.F. Ain, *Adv. Mater. Res.* 620 (2013) 230–235.
8. W. Yang, S. Yu, R. Sun, R. Du, *Ceram. Int.* 38 (2012) 3553–3562.
9. K.H. Felgner, T. Müller, H.T. Langhammer, H.-P. Abicht, *Mater. Lett.* 58 (2004) 1943–1947.
10. U. Diebold, J.F. Anderson, K.-O. Ng, D. Vanderbilt, *Phys. Rev. Lett.* 77 (1996) 1322–1325.
11. R. Schaub, *Science* 299 (2003) 377–379.
12. H.-J. Kim, K.-J. Jeong, D.-S. Bae, *Korean J. Mater. Res.* 22 (2012) 249–252.
13. N. González, M.D.À. Custal, S. Lalaouna, J.R. Riba, E. Armelin, *Eur. Polym. J.* 75 (2016) 210–222.
14. F. Zhang, L. Liao, Y. Wang, Y. Wang, H. Huang, P. Li, Z. Peng, R. Zeng, *J. Rare Earths*. 34 (2016) 221–226.
15. Q.M. Zhang, H. Li, M. Poh, F. Xia, Z.-Y. Cheng, H. Xu, C. Huang, *Nature*. 419 (2002) 284–287.
16. J. Machotova, S. Podzimek, P. Kvasnicka, H. Zgoni, J. Snuparek, M. Cerny, *Prog. Org. Coatings*. 92 (2016) 23–28.
17. H. Jaafar, F.S. Ramle Mhd, M.A. Sulaiman, N.N. Aminuddin, *J. Trop. Resour. Sustain. Sci.* 3 (2015) 30–34.
18. M.A. Sulaiman, S.D. Hutagalung, A. Zainal, *J. Nucl. Relat. Technol.* 10 (2013) 43–52.
19. M.A. Sulaiman, S.D. Hutagalung, M.F. Ain, Z.A. Ahmad, *J. Alloys Compd.* 493 (2010) 486–492.
20. J.N. Hart, Y.-B. Cheng, G.P. Simon, L. Spiccia, *Surf. Coatings Technol.* 198 (2005) 20–23.

© 2016 by the authors. Published by EMS([www.electroactmater.com](http://www.electroactmater.com)). This article is an open access article distributed under the terms and conditions of the Creative Commons Attribution license (<http://creativecommons.org/licenses/by/4.0/>)